

Article

The Origin of the Size Effect in the Oxidation of CO on Supported Palladium Nanoparticles

Vasily V. Kaichev ^{1,*} , Andrey A. Saraev ¹ , Aleksandr V. Fedorov ²  and Evgeny Yu. Gerasimov ¹ 

¹ Department of Catalyst Research, Boreskov Institute of Catalysis, Novosibirsk 630090, Russia; asaraev@catalysis.ru (A.A.S.); gerasimov@catalysis.ru (E.Y.G.)

² Department of Catalyst Discovery and Reaction Engineering, Leibniz-Institut für Katalyse e.V., 18059 Rostock, Germany; aleksandr.fedorov@catalysis.de

* Correspondence: vvk@catalysis.ru

Abstract: Two Pd/TiO₂ catalysts with mean particle sizes of 1 and 3 nm were prepared and tested in the low-temperature oxidation of CO. It was found that the first catalyst with higher dispersion is more active. Turnover frequencies varied for these catalysts by almost six times. In contrast, the apparent activation energy of the oxidation of CO on the catalyst with smaller Pd nanoparticles was estimated at 76 kJ/mol, and for the catalyst with larger Pd nanoparticles at 58 kJ/mol. According to in situ XANES studies, the particle size effect originates from the oxidation of small palladium nanoparticles under reaction conditions, whereas larger nanoparticles are stable and consist of palladium atoms mainly in the metallic state. Palladium oxide is more active in the low-temperature oxidation of CO than metallic palladium. This means that the origin of size-dependent activity of Pd nanoparticles in the low-temperature oxidation of CO is associated with the change in the chemical composition of nanoparticles that leads to a change in the reaction mechanism and, as a result, in their activity.

Keywords: heterogeneous catalysis; size effect; nanoparticles; palladium; CO oxidation



Citation: Kaichev, V.V.; Saraev, A.A.; Fedorov, A.V.; Gerasimov, E.Y. The Origin of the Size Effect in the Oxidation of CO on Supported Palladium Nanoparticles. *Catalysts* **2023**, *13*, 1435. <https://doi.org/10.3390/catal13111435>

Academic Editor: Bo Weng

Received: 1 October 2023

Revised: 28 October 2023

Accepted: 7 November 2023

Published: 13 November 2023



Copyright: © 2023 by the authors. Licensee MDPI, Basel, Switzerland. This article is an open access article distributed under the terms and conditions of the Creative Commons Attribution (CC BY) license (<https://creativecommons.org/licenses/by/4.0/>).

1. Introduction

Numerous studies of heterogeneous catalytic reactions over supported catalysts have shown that the reaction rate per unit surface area of the active phase of the catalyst, which is often expressed as the turnover frequency (TOF [1,2]), can drastically change when the particle size changes between 1 and 10 nm. Boudart suggested calling catalytic reactions with a clear dependence of the TOF on the particle size or crystallographic plane as “structure-sensitive” reactions [1,3]. Accordingly, reactions with no such effect were termed “structure-insensitive”. The rate of structure-sensitive reactions can depend on particle size in different ways; for example, with a decrease in the particle size, the TOF can increase (i.e., smaller nanoparticles are more active than larger ones), decrease (smaller particles are less active), or go through a maximum. Che and Bennet reviewed the effect of the particle size of supported metals on the reaction rate and concluded that in many cases, the size effect can be explained by geometric or electronic factors [4].

A typical example of the size effect in heterogeneous catalysis is observed for Au-based catalysts. For many years, it was believed that gold has a very low activity in catalytic reactions. However, in 1987, Haruta and co-workers demonstrated that highly dispersed gold nanoparticles (NPs) supported on reducible metal oxides such as TiO₂, Fe₂O₃, or Co₃O₄ have extraordinary activity in the low-temperature oxidation of CO [5]. Afterward, it was shown that the rate of this reaction, normalized to an exposed metal surface atom, increases sharply when the particle size decreases below a critical level [6–8]. It was also shown that the particle size (rather than the nature of the support) determines the activity of gold catalysts; Au NPs were active in the CO oxidation even when supported on nonreducible metal oxides such as Al₂O₃ or MgAl₂O₄ [8]. A number of authors believe that

the size effect is associated with the presence of a large number of low-coordinated gold atoms on the surface of Au NPs, which are highly active in the oxidation of CO [9]. This idea was confirmed by XANES measurements, which indicate that there are no electronic effects and all gold atoms in the supported catalysts are in the metallic state [9]. This hypothesis was also confirmed by DFT calculations [9], according to which the adsorption of CO and oxygen does not occur on Au atoms with a coordination number (CN) larger than seven. The calculations showed that the catalytically active centers are gold atoms at the edges (CN = 7) and corners (CN = 5 or 6) of Au NPs, and that their proportion increases with a decrease in the size of the nanoparticles. Recently, a similar “geometric mechanism” has been applied to explain the size effect in the oxidation of methane over supported Pd/Al₂O₃ catalysts. Chen and co-workers showed that the rate of methane oxidation normalized to the number of active surface sites monotonically increases by approximately six times when the size of Pd NPs decreases from 10 to 2 nm [10]. The authors associated the increase in the reaction rate with increasing the number of corners on the surface of the nanoparticles and decreasing their size [11]. This effect was confirmed by the results of DFT calculations [10], which indicated that the methane molecule is much more easily activated at the corner sites of Pd NPs than on other sites (i.e., edges or terraces).

Herein, we focus on studying the particle size effect in the oxidation of CO over Pd-based catalysts. Initially, this reaction was considered as structure-insensitive because it does not depend on the structure of the crystal surface [12]. Moreover, Ladas and co-workers [13], who tested the oxidation of CO over Pd NPs supported on an α -Al₂O₃ single crystal under oxygen-rich conditions ($P_{O_2}/P_{CO} = 1.1$), found that the turnover frequency at 172 °C does not change when the particle size varies from 1.5 to 8 nm. However, at 245 °C, the TOF remained approximately constant for particles larger than 4 nm, and then increased almost three-fold for 1.5 nm particles. Such unusual behavior cannot be explained in terms of simple geometric or electronic models [4].

2. Results and Discussion

To elucidate the origin of the size-dependent activity in the low-temperature oxidation of CO, we prepared two Pd/TiO₂ supported catalysts with mean particle sizes of approximately 1 and 3 nm, respectively. According to X-ray fluorescence analysis, the total metal loading was 1 wt% in both catalysts. The catalysts were referred to as Pd-1 and Pd-3, respectively. Typical HRTEM images of the catalysts and corresponding particle size distribution histograms are presented in Figure 1. As seen, both catalysts are characterized by a narrow particle size distribution, and the mean particle diameters of Pd-1 and Pd-3 were 0.8 and 3.3 nm, respectively.

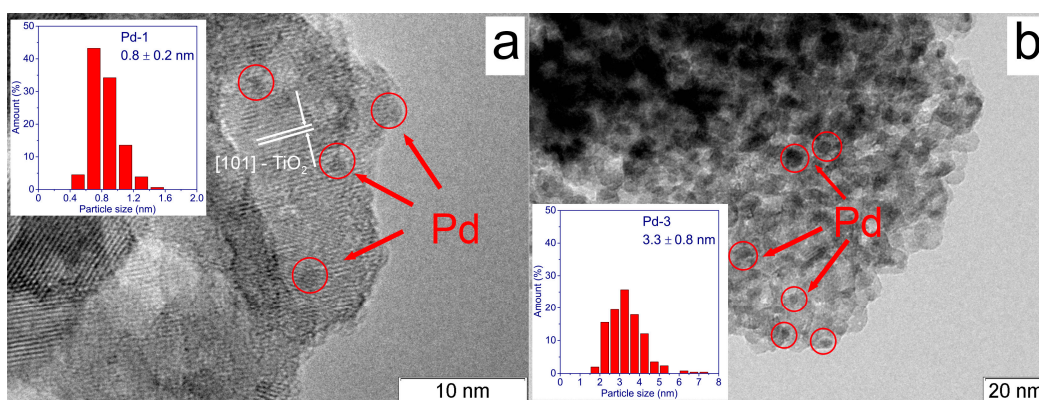


Figure 1. High-resolution transmission electron microscopy images of the Pd/TiO₂ catalysts with a mean particle size of approximately 1 nm (a) and 3 nm (b). Particle size distributions are presented in the insets.

The catalytic activity of the Pd/TiO₂ catalysts in the low-temperature oxidation of CO was tested in a gradientless flow-circulation reactor. The experiments were performed at atmospheric pressure under oxygen-rich conditions ($P_{O_2}/P_{CO} = 10$). The main results are summarized in Table 1. It was found that the Pd-1 catalyst is more active than the Pd-3 catalyst. The rate of CO oxidation for these catalysts differed by almost nine times at 85 °C and the turnover frequency was 0.140 and 0.022 s⁻¹, respectively. The TOFs were calculated by normalization of the reaction rate to the number of active sites on the catalyst surface, and the number of active sites was determined by pulse chemisorption of CO.

Table 1. Mean diameter of Pd NPs (d) obtained from HRTEM data, rate of CO oxidation (r_{CO}^*) measured at 85 °C at CO conversion of 50%, number of metal atoms on the catalyst surface (N_s) calculated from CO chemisorption data, apparent activation energy (E_a), and calculated TOFs for the Pd-based catalysts under study.

Catalyst	d , nm	r_{CO}	N_s , $\mu\text{mol/g}$	E_a , kJ/mol	TOF, s ⁻¹
Pd-1	0.8	6.88	49.5	76 ± 4	0.14
Pd-3	3.3	0.78	34.8	58 ± 4	0.022

Figure 2 shows the Arrhenius plots of the oxidation of CO. The results disclose a much higher apparent activation energy for the Pd-1 catalyst (76 kJ/mol) than for the Pd-3 catalyst (58 kJ/mol). The latter value is in good agreement with the results by Meusel and co-workers, who studied the oxidation of CO over alumina supported Pd NPs by the molecular beam technique [14]. They showed that the apparent activation energy for the low-temperature oxidation of CO over metallic Pd NPs with a mean size of 5.5 nm is 57–62 kJ/mol, which is close to the energy observed for the oxidation of CO over a Pd(111) single crystal under ultrahigh vacuum conditions [14].

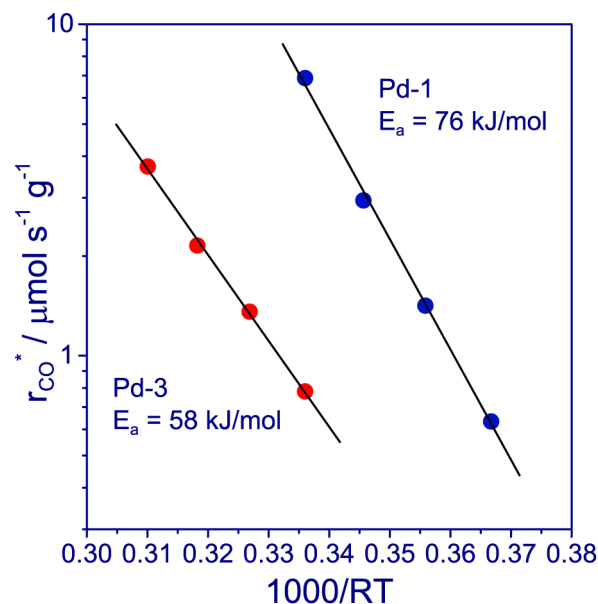


Figure 2. Logarithmic reaction rate of the oxidation of CO over Pd/TiO₂ catalysts as a function of reciprocal temperature under oxygen-rich conditions. The reaction feed consists of 1 vol.% CO, 10 vol.% O₂, and the balance Ar. The total pressure is 1 bar. The technical details are presented in SI.

The large difference in the apparent activation energies observed in our experiments indicates that the oxidation of CO over these Pd/TiO₂ catalysts proceeds differently. As it is generally believed, the reaction mechanism of the oxidation of CO over palladium strongly depends on its chemical state. Most researchers assume that if palladium is in the metallic state, the reaction proceeds via the Langmuir–Hinshelwood (LH) mechanism (see

Ref. [14] and references therein). In this case, both CO and O₂ are adsorbed on the metallic surface, oxygen dissociates to form two O_{ads}, and then the O_{ads} reacts with CO_{ads} to form CO₂. Alternatively, the reaction over metallic palladium can proceed via the Eley–Rideal mechanism, when CO molecules from the gas phase hit the surface and directly react with the adsorbed oxygen species [15]. However, this mechanism is rarely implemented in practice. At the same time, palladium can be oxidized to PdO under oxygen-rich conditions, and the reaction can proceed on the oxidized catalyst's surface via a two-step redox mechanism [15]. In the first step, CO reacts with palladium oxide to form CO₂ and an oxygen vacancy. In the second step, the catalyst's surface is restored by filling the oxygen vacancy with O₂ from the gas phase. This mechanism is often referred to as the Mars–van Krevelen (MvK) mechanism [16]. Obviously, the LH and MvK mechanisms differ in the nature of active oxygen species. The LH mechanism suggests that CO is oxidized by adsorbed oxygen species, whereas in the MvK mechanism CO reacts with lattice oxygen species. As a result, the activation barrier for the CO oxidation may differ. Hence, the size effect in the low-temperature oxidation of CO over the Pd/TiO₂ catalysts may originate from a change in the chemical state of supported palladium.

To verify this hypothesis, the Pd/TiO₂ catalysts were studied in situ under a flow of a CO/O₂ mixture by XANES. The experiments were performed at atmospheric pressure using a capillary-based flow microreactor. The reaction gas feed contained 1 vol.% CO and 10 vol.% O₂ in helium. Before the in situ studies, the catalysts were reduced in a mixture of H₂ in helium at 300 °C for 30 min. The Pd K-edge XANES spectra of the reduced and working Pd/TiO₂ catalysts, as well as the spectra of Pd foil and bulk PdO, are presented in Figure 3. As seen, the spectrum of bulk palladium in the metallic state (Pd foil, curve 1) consists of three peaks: two well-resolved peaks at 24,367.7 and 24,391.6 eV and a peak at 24,430.5 eV with a well-pronounced shoulder at 24,412.4 eV. The first two absorption maxima are assigned to final states of 5*p* and 4*f* type characters, respectively [17–19]. The spectrum of the reduced Pd-3 catalyst contains the same peaks at 24,369.1 and 24,390.0 eV and a peak at 24,429.5 eV with a weak shoulder at 24,414.4 eV (Figure 3, curve 2). In turn, the spectrum of the reduced Pd-1 catalyst has a slightly different shape and contains three well-resolved peaks at 24,367.2, 24,389.4, and 24,427.0 eV (Figure 3, curve 4). In full agreement with theoretical calculations [17], the 4*f* peak of the reduced catalysts is shifted by 1.6–2.2 eV compared to that of bulk Pd. A similar effect has been observed for palladium carbide [19], where the 4*f* peak was shifted to lower energies due to an expansion of the crystal lattice compared to pure metallic Pd. Palladium carbide (PdC_x, *x* < 0.15) is formed by the dissolution of carbon atoms in the lattice of palladium metal. Hence, the spectra in Figure 3 show that palladium in both of our reduced catalysts is mainly in the metallic state.

The Pd K-edge XANES spectra of the Pd/TiO₂ catalysts obtained in situ in the CO/O₂ mixture at 150 °C are significantly different. The spectrum of Pd-3 (Figure 3, curve 3) is almost identical to the spectrum obtained in hydrogen, indicating that the chemical state of palladium in 3-nm NPs does not change during the oxidation of CO. The spectrum contains the same peaks at 24,369.0 and 24,390.6 eV and a peak at 24,430.2 eV with a weak shoulder at 24,413.7 eV. In contrast, the spectrum of Pd-1 (Figure 3, curve 5) is shifted to higher energies and its shape changes markedly. The threshold energy (*E*₀) determined as the first inflection point on the rising edge of the Pd K-edge spectrum is 24,350.5 and 24,355.0 eV for the reduced and working Pd-1 catalysts, respectively. The first value is closer to the threshold energy characteristic of palladium in the metallic state (24,350.0 eV), while the second coincides with the value observed for bulk PdO (24,355.0 eV). Moreover, the spectrum of Pd-1 after the treatment in the CO/O₂ mixture changes and becomes similar to the spectrum of palladium oxide. Indeed, the Pd K-edge XANES spectrum of bulk PdO (Figure 3, curve 6) contains a strong peak at 24,367.5 with a well-pronounced shoulder from the higher energy side as well as two separated peaks at 24,427.3 and 24,451.0 eV. The first peak corresponds to the transition from the 1*s* level to the 5*p*_σ (*e*_u) orbital, while the shoulder may be related to the shake-up process involving Pd 4*d* → 5*p* transitions [20]. The origin of the other peaks is not clear yet. The spectrum of the Pd-1 catalyst obtained in situ

in the CO/O₂ mixture (Figure 3, curve 5) contains a strong asymmetric peak at 24,370.4 eV and an additional peak at 24,431.7 eV. These peaks show that palladium in the Pd-1 catalyst is oxidized under the reaction conditions. The minor differences between the spectra of PdO and oxidized Pd-1 indicate that the structure of palladium oxide formed during the oxidation of palladium nanoparticles with a size of 1 nm slightly differs from the structure of bulk PdO.

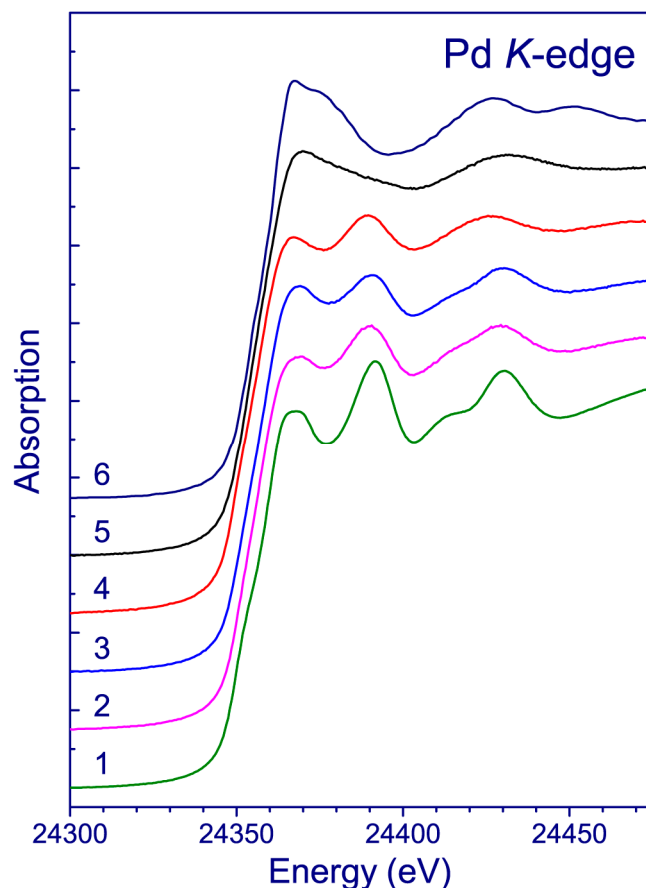


Figure 3. Normalized Pd K-edge XANES spectra of Pd foil (1) and bulk PdO (6) obtained at room temperature; reduced Pd-3 (2) and Pd-1 (4) catalysts obtained in situ in H₂/He mixture at 300 °C; and working Pd-3 (3) and Pd-1 (5) catalysts obtained in situ in CO/O₂/He mixture at 150 °C. The calibration was performed by setting the first inflection point on the rising edge of the Pd K-edge spectrum of Pd foil at 24,350.0 eV.

This finding agrees well with the results by Hendriksen and co-workers [21], who studied self-sustained oscillations in the catalytic oxidation of CO over a Pd(001) single crystal using X-ray diffraction (XRD) and mass spectrometry. They found that the oscillations arise due to reversible oxidation and reduction of palladium. The surface of metallic palladium has a low activity, but the growth of a thin oxide film on the palladium surface leads to an increase in activity. The authors also suggest that the oxidation of CO on the surface of metallic palladium proceeds via the LH mechanism, whereas on the surface of PdO the reaction proceeds via the MvK mechanism. Again, Baylet and co-workers [22] showed that the smaller Pd NPs are more easily oxidized at lower temperatures than the larger ones.

Taking into account these data and our results, we can conclude that the enhanced activity of small Pd NPs in the low-temperature oxidation of CO is determined by their oxidation under reaction conditions. This means that the origin of size effect in the oxidation of CO on the Pd-based catalysts is caused by the change in the chemical composition of the Pd NPs with a size of approximately 1 nm. Small palladium nanoparticles are oxidized

under reaction conditions, whereas larger nanoparticles are stable and consist of palladium atoms mainly in the metallic state. The change in the chemical composition of nanoparticles leads to a change in the reaction mechanism and, as a result, in the reaction activation barrier. The obtained results show that palladium oxide is more active in the low-temperature oxidation of CO than metallic palladium. To the best of our knowledge, such a redox model of the size effect has not yet been discussed in the literature.

This model can be applied to some other catalytic systems, such as the oxidation of CO over Pt/TiO₂ catalysts, where a similar positive size effect has been observed. As shown by Li and co-workers, a decrease in the Pt particle size from 10 to 1 nm leads to an increase in the TOF by a factor of about seven [23]. However, it should be noted that this model is not universal because the oxidation and reduction of transition metals can affect their catalytic activity in different ways. For example, it has been recently shown by operando XRD studies that metallic palladium is more active than PdO in the oxidation of methane [24]. Therefore, the size effect in the oxidation of methane on Pd-based catalysts cannot be associated with the oxidation of small nanoparticles under reaction conditions. As shown by Chen and co-workers, the size effect in this catalytic system can be explained by the geometric model [10]. Again, researchers from Somorjai's group found the opposite size effect in the oxidation of CO on Ru-based catalysts under oxygen-rich conditions; the CO oxidation activity increases with the NP size. They showed that their 6 nm Ru NPs catalyst shows an eight-fold higher activity than their 2 nm catalyst [25]. The authors associated the enhanced activity of large nanoparticles with the formation of a core-shell structure where an active RuO₂ shell layer is formed on an Ru metallic core.

3. Materials and Methods

3.1. Catalyst Preparation

All commercial reagents used were of analytical grade without further purification. To prepare Pd/TiO₂ catalysts with different Pd particle sizes, we applied two different deposition–precipitation techniques based on the use of polyoxometalates as reducing and stabilizing agents [26–28]. As a support material, we used commercial Hombifine N TiO₂ (Sachtleben Chemie GmbH, Duisburg, Germany), which is nanometer-scale anatase with the specific surface area of 350 m²/g. The technique details are described elsewhere [26]. In short, palladium was deposited on TiO₂ by sorption using two types of aqueous metal sol. The first catalyst was prepared using a sol containing palladium polyhydroxocomplexes stabilized with Nb-based polyoxometalates. In this case, K₇HNb₆O₁₉·nH₂O was dissolved in distilled water, and an 0.1 M solution of NaOH was added dropwise until its pH was 11.7. This solution was mixed with an aqueous solution of K₂PdCl₄ and then mixed with the TiO₂ powder. The mixture was stirred for 3 h. After that, the prepared solid catalyst was filtered and then washed with distilled water. The solid was first dried at room temperature for 12 h and then dried in an oven at 140 °C for 1 h. In addition, the catalyst was treated in hydrogen at 350 °C for 2 h. This catalyst was referred to as Pd-1. In the second case, the sol contained metal nanoparticles that were stabilized with W-based polyoxometalates. The sol was prepared by mixing aqueous solutions of K₂PdCl₄ and Na₂WO₄·2H₂O. Then, palladium was reduced by bubbling hydrogen through the solution at room temperature. After that, the sol was mixed with the TiO₂ powder and stirred for 3 h. The prepared solid catalyst was filtered and then washed with distilled water. The solid was first dried at room temperature for 12 h and then dried in an oven at 140 °C for 1 h. This catalyst was referred to as Pd-3. According to X-ray fluorescence analysis, the total metal loading was 1 wt% in both Pd/TiO₂ catalysts. TEM images and corresponding size distribution histograms are presented in Figure 1. The specific surface area of the catalysts was approximately 150 m²/g. The latter is due to the low thermal stability of titania and the sintering of titania nanoparticles when drying the catalysts. This effect is often observed for catalysts based on titanium dioxide [26,29].

3.2. Catalyst Study

The catalysts were studied by high-resolution transmission electron microscopy (HRTEM) using a JEOL JEM-2010 electron microscope (JEOL Ltd., Tokyo, Japan). The microscope was operated at 200 kV accelerating voltage that provided a lattice resolution of 0.14 nm. The samples for the HRTEM study were prepared by ultrasonic dispersion in an ethanol suspension and then depositing droplets of the suspension on copper grids coated with a holey amorphous carbon film.

In situ X-ray absorption spectroscopy studies were carried out at Beamline P64 at the high-brilliance storage ring PETRA III at DESY (Hamburg, Germany). The storage ring was operated at 6 GeV with a constant ring current of 100 mA. The experimental station was described in detail elsewhere [30]. In short, the synchrotron radiation was provided by a 90 pole undulator. The radiation was monochromatized using a double-crystal monochromator with Si(311) crystals. To reduce higher harmonics, two silicon X-ray mirrors were used. The monochromator was calibrated by setting the first inflection point on the rising edge of the Pd K-edge spectrum of palladium foil at 24,350.0 eV [19,31]. Note that the first inflection point occurs on the rising edge of an unresolved shoulder that extends to $\mu x \sim 0.5$ at $E - E_0 \sim 5$ eV. The structure within the edge is more obvious in the first derivative of the XANES spectrum. The Pd K-edge XANES spectrum of the Pd foil and the first derivative plot of the spectrum are presented in Figure S1.

The in situ measurements were performed under atmospheric pressure using a capillary-based flow microreactor [32,33]. The microreactor consisted of a quartz glass capillary tube (diameter 1 mm, length 50 mm, wall thickness 0.05 mm) connected to stainless-steel gas lines via stainless-steel gas-tight Swagelok fittings. The catalyst powder was placed into the central part of the capillary and fixed with two quartz wool plugs to form the catalyst bed. The length of the catalyst bed was approximately 10 mm. The capillary was heated with a hot-air blower with a controlled air flow. Before in situ measurements, the catalysts were reduced in a gas mixture of 10 vol.% H₂ in helium at 300 °C for 30 min, followed by cooling to room temperature directly in the reactor. Subsequently, the H₂ flow was stopped, a gas mixture of 1 vol.% CO and 10 vol.% O₂ in helium was introduced into the reactor, and the central part of the capillary was heated to 150 °C. The gas flows were regulated with mass-flow controllers (Bronkhorst High-Tech B.V., Ruurlo, The Netherlands). The total flow rate was 10 sccm in all the experiments. The in situ XAS spectra were acquired in the middle of the catalyst bed. The Pd K-edge X-ray absorption spectra of the Pd/TiO₂ catalysts were obtained in the fluorescence mode using a PIPS detector. Simultaneously, for calibration, the spectra of the palladium foil were collected in transmission mode at room temperature in air using ionization chambers. The XAS data were processed using the Athena program from the Demeter software package 0.9.25 [34,35].

3.3. Catalytic Activity Tests

The catalytic tests were carried out using a gradientless reactor with a flow-circulating configuration at atmospheric pressure [36]. The reactor consisted of a stainless steel tube with a 25 mm inner diameter and a 75 mm length. The reactor was placed inside an electrical oven. The temperature was controlled with a K-type thermocouple attached to the external wall of the reactor. A fraction of the catalyst powder contained grains in the range of 0.2–0.6 mm. The catalyst loading was 1 g. The reactor was equipped with an external circulation pump that provided the constant space velocity of premixed reactants through the catalyst bed with more than 15 recirculations per minute; this provided the total mixing mode and the absence of temperature and concentration gradients. The reaction feed consisted of 1 vol.% CO, 10 vol.% O₂, and the balance Ar. The gas flows were regulated separately with SEC-Z500 mass-flow controllers (Horiba Ltd., Kyoto, Japan). The space velocity of the feed was varied in the experiments from 100 to 1000 mL/min. A TEST-1 gas analyzer (BONER, Novosibirsk, Russia) equipped with an optical absorption infrared sensor was used for analysis of the gas phase at the reactor outlet. A detailed description of

the procedures for calculating the reaction rate and activation energy of the oxidation of CO is provided in the Supplementary Materials.

4. Conclusions

To sum up, the present study demonstrates that the size effect in heterogeneous catalytic reactions cannot always be explained within the framework of simple geometric models. To elucidate the causes of the size effect, at least in oxidative reactions, it is necessary to study the chemical state of supported metals and the atomic structure of nanoparticles using in situ/operando methods at ambient pressures. Supported metal nanoparticles can undergo oxidation under the influence of the reaction medium, which in turn can lead to a change in the reaction mechanism and the actual activity of the catalyst. Such an effect is realized in the low-temperature oxidation of CO over Pd/TiO₂ catalysts, where the catalysts with Pd NPs with a size of approximately 1 nm are more active. According to in situ XANES studies, the particle size effect originates from the oxidation of small palladium nanoparticles under reaction conditions, whereas larger nanoparticles remain stable and consist of palladium mainly in the metallic state. PdO is more active in the low-temperature oxidation of CO than metallic palladium.

Supplementary Materials: The following supporting information can be downloaded at <https://www.mdpi.com/article/10.3390/catal13111435/s1>, Figure S1: The Pd K-edge XANES spectrum of Pd foil. The first derivative plot of the spectrum is presented in the inset; Figure S2: Correlations between the rate of CO oxidation and CO conversion for the Pd-3 (left) and Pd-1 (right) catalysts at different reaction temperatures.

Author Contributions: Conceptualization, V.V.K.; methodology, V.V.K., A.A.S. and A.V.F.; experimental testing, A.A.S., A.V.F. and E.Y.G.; data analysis, A.A.S., A.V.F. and E.Y.G.; writing—original draft, V.V.K.; writing—review and editing, V.V.K.; supervision, V.V.K. All authors have read and agreed to the published version of the manuscript.

Funding: This work was supported by the Ministry of Science and Higher Education of the Russian Federation (Agreement No. 075-15-2022-263).

Data Availability Statement: The raw data are not publicly available at this time but may be obtained from the authors upon reasonable request.

Acknowledgments: The authors are grateful to Dmitry Ermakov for the catalyst testing. The authors also thank Vadim Murzin, Anna Kremneva, and Olga Bulavchenko for their assistance in the XANES experiments and the staff of DESY for their support during the beamline operation. The investigations were performed in part using the large-scale research facilities, including the “EXAFS spectroscopy beamline”, at the Siberian Synchrotron and Terahertz Radiation Center.

Conflicts of Interest: The authors declare no conflict of interest.

References

1. Boudart, M.; Aldag, A.; Benson, J.E.; Dougharty, N.A.; Girvin Harkins, C. On the specific activity of platinum catalysts. *J. Catal.* **1966**, *6*, 92–99. [[CrossRef](#)]
2. Kozuch, S.; Martin, J.M.L. “Turning over” definitions in catalytic cycles. *ACS Catal.* **2012**, *2*, 2787–2794. [[CrossRef](#)]
3. Boudart, M. Catalysis by supported metals. *Adv. Catal.* **1969**, *20*, 153–166.
4. Che, M.; Bennett, C.O. The influence of particle size on the catalytic properties of supported metals. *Adv. Catal.* **1989**, *36*, 55–172.
5. Haruta, M.; Koboyashi, T.; Sano, H.; Yamada, N. Novel gold catalysts for the oxidation of carbon monoxide at a temperature far below 0 °C. *Chem. Lett.* **1987**, *16*, 405–408. [[CrossRef](#)]
6. Haruta, M.; Tsubota, S.; Kobayashi, T.; Kageyama, H.; Genet, M.J.; Delmon, B. Low-temperature oxidation of CO over gold supported on TiO₂, α-Fe₂O₃, and Co₃O₄. *J. Catal.* **1993**, *144*, 175–192. [[CrossRef](#)]
7. Emmanuel, J.; Hayden, B.E.; Saleh-Subaie, J. The particle size dependence of CO oxidation on model planar titania supported gold catalysts measured by parallel thermographic imaging. *J. Catal.* **2019**, *369*, 175–180. [[CrossRef](#)]
8. Lopez, N.; Janssens, T.V.W.; Clausen, B.S.; Xu, Y.; Mavrikakis, M.; Bligaard, T.; Nørskov, J.K. On the origin of the catalytic activity of gold nanoparticles for low-temperature CO oxidation. *J. Catal.* **2004**, *223*, 232–235. [[CrossRef](#)]
9. Janssens, T.V.W.; Clausen, B.S.; Hvolbæk, B.; Falsig, H.; Christensen, C.H.; Bligaard, T.; Nørskov, J.K. Insights into the reactivity of supported Au nanoparticles: Combining theory and experiments. *Top. Catal.* **2007**, *44*, 15–26. [[CrossRef](#)]

10. Chen, J.; Zhong, J.; Wu, Y.; Hu, W.; Qu, P.; Xiao, X.; Zhang, G.; Liu, X.; Jiao, Y.; Zhong, L.; et al. Particle size effects in stoichiometric methane combustion: Structure–activity relationship of Pd catalyst supported on gamma-alumina. *ACS Catal.* **2020**, *10*, 10339–10349. [[CrossRef](#)]
11. Van Hardeveld, R.; Hartog, F. The statistics of surface atoms and surface sites on metal crystals. *Surf. Sci.* **1969**, *15*, 189–230. [[CrossRef](#)]
12. Engel, T.; Ertl, G. Elementary steps in the catalytic oxidation of carbon monoxide on platinum metals. *Adv. Catal.* **1979**, *28*, 3214–3217.
13. Ladas, S.; Poppa, H.; Boudart, M. The adsorption and catalytic oxidation of carbon monoxide on evaporated palladium particles. *Surf. Sci.* **1981**, *102*, 151–171. [[CrossRef](#)]
14. Meusel, I.; Hoffmann, J.; Hartmann, J.; Heemeier, M.; Bäumer, M.; Libuda, J.; Freund, H.-J. The interaction of oxygen with alumina-supported palladium particles. *Catal. Lett.* **2001**, *71*, 5–13. [[CrossRef](#)]
15. Van Spronsen, M.A.; Frenken, J.W.M.; Groot, I.M.N. Surface science under reaction conditions: CO oxidation on Pt and Pd model catalysts. *Chem. Soc. Rev.* **2017**, *46*, 4347–4374. [[CrossRef](#)]
16. Mars, P.; Van Krevelen, D.W. Oxidations carried out by the means of vanadium oxide catalysts. *Chem. Eng. Sci.* **1954**, *3*, 41–59. [[CrossRef](#)]
17. Nilsson, J.; Carlsson, P.-A.; Grönbeck, H.; Skoglundh, M. First principles calculations of palladium nanoparticle XANES spectra. *Top. Catal.* **2017**, *60*, 283–288. [[CrossRef](#)]
18. Muller, J.E.; Jepsen, O.; Andersen, O.K.; Wilkins, J.W. Systematic structure in the K-edge photoabsorption spectra of the 4d transition metals: Theory. *Phys. Rev. Lett.* **1978**, *40*, 720–722. [[CrossRef](#)]
19. McCauley, J.A. Temperature dependence of the Pd K-edge extended x-ray-absorption fine structure of PdC_x (x~0.13). *Phys. Rev. B* **1993**, *47*, 4873–4879. [[CrossRef](#)]
20. Kim, S.-J.; Lemaux, S.; Demazeau, G.; Kim, J.-Y.; Choy, J.-H. X-Ray absorption spectroscopic study on LaPdO₃. *J. Mater. Chem.* **2002**, *12*, 995–1000. [[CrossRef](#)]
21. Hendriksen, B.L.M.; Ackermann, M.D.; Van Rijn, R.; Stoltz, D.; Popa, I.; Balmes, O.; Resta, A.; Wermeille, D.; Felici, R.; Ferrer, S.; et al. The role of steps in surface catalysis and reaction oscillations. *Nature Chem.* **2010**, *2*, 730–734. [[CrossRef](#)] [[PubMed](#)]
22. Baylet, A.; Marecot, P.; Duprez, D.; Castellazzi, P.; Groppi, G.; Forzatti, P. In situ Raman and in situ XRD analysis of PdO reduction and Pd⁰ oxidation supported on γ -Al₂O₃ catalyst under different atmospheres. *Phys. Chem. Chem. Phys.* **2011**, *13*, 4607–4613. [[CrossRef](#)] [[PubMed](#)]
23. Li, N.; Chen, Q.-Y.; Luo, L.-F.; Huang, W.-X.; Luo, M.-F.; Hu, G.-S.; Lu, J.-Q. Kinetic study and the effect of particle size on low temperature CO oxidation over Pt/TiO₂ catalysts. *Appl. Catal. B* **2013**, *142–143*, 523–532. [[CrossRef](#)]
24. Kaichev, V.V.; Vinokurov, Z.S.; Saraev, A.A. Self-sustained oscillations in oxidation of methane over palladium: The nature of “low-active” and “highly active” states. *Catal. Sci. Technol.* **2021**, *11*, 4392–4397. [[CrossRef](#)]
25. Joo, S.H.; Park, J.Y.; Renzas, J.R.; Butcher, D.R.; Huang, W.; Somorjai, G.A. Size effect of ruthenium nanoparticles in catalytic carbon monoxide oxidation. *Nano Lett.* **2010**, *10*, 2709–2713. [[CrossRef](#)]
26. Maksimov, G.M.; Gerasimov, E.Y.; Kenzhin, R.M.; Saraev, A.A.; Kaichev, V.V.; Vedyagin, A.A. CO oxidation over titania-supported gold catalysts obtained using polyoxometalate. *Reac. Kinet. Mech. Catal.* **2021**, *132*, 171–185. [[CrossRef](#)]
27. Keita, B.; Liu, T.; Nadjo, L. Synthesis of remarkably stabilized metal nanostructures using polyoxometalates. *J. Mater. Chem.* **2009**, *19*, 19–33. [[CrossRef](#)]
28. Wang, Y.; Weinstock, I.A. Polyoxometalate-decorated nanoparticles. *Chem. Soc. Rev.* **2012**, *41*, 7479–7496. [[CrossRef](#)]
29. Andrushkevich, T.V.; Kaichev, V.V.; Chesalov, Y.A.; Saraev, A.A.; Bukhtiyarov, V.I. Selective oxidation of ethanol over vanadia-based catalysts: The influence of support material and reaction mechanism. *Catal. Today* **2017**, *279*, 95–106. [[CrossRef](#)]
30. Caliebe, W.A.; Murzin, V.; Kalinko, A.; Gorlitz, M. High-flux XAFS-Beamline P64 at PETRA III. *AIP Conf. Proc.* **2019**, *2054*, 060031.
31. Bearden, J.A.; Burr, A.F. Reevaluation of X-ray atomic energy levels. *Rev. Mod. Phys.* **1967**, *39*, 125–142. [[CrossRef](#)]
32. Clausen, B.S.; Steffensen, G.; Fabius, B.; Villadsen, J.; Feidenhans'l, R.; Topsøe, H. In situ cell for combined XRD and on-line catalysis tests: Studies of Cu-based water gas shift and methanol catalysts. *J. Catal.* **1991**, *132*, 524–535. [[CrossRef](#)]
33. Grunwaldt, J.-D.; Caravati, M.; Hannemann, S.; Baiker, A. X-ray absorption spectroscopy under reaction conditions: Suitability of different reaction cells for combined catalyst characterization and time-resolved studies. *Phys. Chem. Chem. Phys.* **2004**, *6*, 3037–3047. [[CrossRef](#)]
34. Newville, M. IFEFFIT: Interactive XAFS analysis and FEFF fitting. *J. Synchrotron Rad.* **2001**, *8*, 322–324. [[CrossRef](#)] [[PubMed](#)]
35. Ravel, B.; Newville, M. ATHEAN, ARTERMIS, HEPHAESTUS: Data analysis for X-ray absorption spectroscopy using IFEFFIT. *J. Synchrotron. Rad.* **2005**, *12*, 537–541. [[CrossRef](#)]
36. Fedorov, A.; Saraev, A.; Kremneva, A.; Selivanova, A.; Vorokhta, M.; Šmíd, B.; Bulavchenko, O.; Yakovlev, V.; Kaichev, V. Kinetic and mechanistic study of CO oxidation over nanocomposite Cu–Fe–Al oxide catalysts. *ChemCatChem* **2020**, *12*, 4911–4921. [[CrossRef](#)]

Disclaimer/Publisher’s Note: The statements, opinions and data contained in all publications are solely those of the individual author(s) and contributor(s) and not of MDPI and/or the editor(s). MDPI and/or the editor(s) disclaim responsibility for any injury to people or property resulting from any ideas, methods, instructions or products referred to in the content.